Assembly meshing of abrasive waterjet nozzle erosion simulation

Assembly meshing of abrasive waterjet nozzle erosion simulation

N H Kamarudin[1], A Mebrahitom[1] and A Azhari [1]

[1]Department of Manufacturing, Universiti Malaysia Pahang (UMP), 26600 Pekan, Pahang Malaysia

Email:naqibhbk@gmail.com

Abstract. Computational Fluid Dynamics (CFD) softwares have been prevalent in Abrasive Waterjet (AWJ) Modelling for optimization and prediction. However, there are many different methods in approaching a single problem especially in predicting the erosion rate of nozzle which is critical in influencing kerf quality of AWJ cutting. In this paper, three main methods of assembly meshing for an abrasive waterjet erosion were simulated which is Quadrilateral, Cutcell and Tetrahedrons and each processing time, quality of convergence and accuracy of results are discussed. Results shows that Quadrilateral mesh prevails in the mentioned category followed by Tetrahedrons and Cutcell.

1. Introduction

Computational Fluid Dynamics (CFD) is a technique to solve and analyze problems that involves fluid flows using numerical methods and algorithms. Using computers to perform modeling, simulations and analysis of fluid flow enables CFD practitioners to have insights of flow patterns that have been difficult to be performed using traditional experimental techniques. Currently, CFD applications can be found in the field of aerospace, turbo machinery, automotive and maritime. The capabilities of CFD also made it way in meteorology, oceanography, astrophysics, oil recovery and architecture. A comprehensive explanation of CFD principles and applications have been done by Blazek [1], Versteeg and Malalasekera [2] and Anderson and Wendt [3]. Currently, the development of CFD software has been very promising. ANSYS Fluent software is well known and widely used CFD engineering software for modeling fluid flow. Abrasive Waterjet (AWJ) Machine have been known for its versatility and widely used in the industry for multiple fabrication process and cleaning [4-6]. An AWJ related study was conducted by Junkar, Jurisevic, Fajdiga and Grah [7] to study the effect of erosion impact of a single particle abrasive with the target workpiece which is stainless steel (AISI 304). The research was done using LS Dyna where the crater spherity in the simulation was used to compare with the observation of experimental shapes of craters on the workpiece material. The study is emphasized only in the measurements of the sphericity of the impact crater and limited parameters of abrasive and workpiece material.

Maniadaki, Kestis, Bilalis and Antoniadis [8] proposed a finite element-based model for pure waterjet process simulation and the main objective was to investigate and analyse in detail the material behaviour of a work piece under waterjet impingement. The model developed using LS-DYNA 3D code to simulates the erosion of the target material caused by the high-pressure waterjet flow.

Maniadaki, Kestis, Bilalis and Antoniadis [8] proposed a finite element-based model for pure waterjet process simulation and the main objective was to investigate and analyse in detail the material behaviour of a work piece under waterjet impingement. The model developed using LS-DYNA 3D code to simulates the erosion of the target material caused by the high-pressure waterjet flow.

Deepak, Anjaiah, Karanth and Sharma [9] had also used ANSYS software to examine the effect of inlet pressure on skin friction coefficient and jet exit kinetic energy. Per the results, the effect of increasing the inlet pressure causes significant increase to the skin coefficient friction and increased in the jet kinetic energy correspondingly. Further analysis then suggested that by increasing the volume fraction of abrasives causes a significant decrease on both skin coefficient friction and jet kinetic energy.

Baisheng, Hui, Lei, Jufeng, Hua, Zhen, Longkang and Hailong [10] have performed numerical simulation of the flow field of abrasive waterjet nozzle under submerging conditions based on FLUENT software. The research used RNG κ-ε turbulent model and simple algorithm for simulation to simulate flow field from generated from an abrasive waterjet nozzle. The research indicated that there are three zones which are free jet zone, shock zone and wall jet zone. Shock zone suggest the distance for the best cutting distance which is shown to be within the scope of 2 – 7 times the nozzle exit diameter.

Deepak, Anjaiah, Karanth and Sharma [9] had also applied CFD in AWJ to examine the effect of inlet pressure on skin friction coefficient and jet exit kinetic energy of the AWJ nozzle. Per the results, the effect of increasing the inlet pressure causes significant increase to the skin coefficient friction and increased in the jet kinetic energy correspondingly. Further analysis then suggested that by increasing the volume fraction of abrasives causes a significant decrease on both skin coefficient friction and jet kinetic energy. It is noted that the research does not undertake erosion studies of the nozzle.

On the other hand, studies using CFD in investigating erosion in AWJ nozzle are very limited. Mostofa, Kil and Hwan [11] used the ANSYS CFX software to simulate multiphase flow of water, air and abrasives in the mixing tube to monitor erosion rate at the mixing tube wall and predict the influence of abrasive particle size with different parameters of tube lengths. The erosion model is based on Finnie's erosion model of ductile material. The result showed that abrasive shape and jet velocity have effect on erosion rate. The erosion rate has similar linear results as obtained by Nanduri, Taggart and Kim [12]. Further CFD based for AWJ studies was conducted by Kamarudin, Rao and Azhari [13] by using Discrete Phase Method (DPM) to predict the erosion of AWJ nozzle. Present study shows how different the results of the erosion rate of the nozzle affected by manipulating the assembly of the mesh. The information for the processing time and convergence are also added to provide alternative options for the best method of AWJ simulation.

Assumptions and Theoretical Formulation

The flow is assumed to be multiphase and the fluid is treated as continuum and incompressible. The particle's abrasive velocity is assumed to be the same as those of flowing fluid. The Langrangian-Eulerian model was used to solve the coupling of the fluid flow and abrasives, also called discrete particle modeling, which solves the equations of motion individually for each particle, whereby the continuous phase is modeled using a Eulerian framework and the trajectories of the particles are simulated within a Lagrangian framework. In a two-way coupling, each particle exchanges mass, momentum and energy with the fluid phase valid for the current work [9], [14]-[17]. The theoretical waterjet velocity was used by Mostofa, Kil and Hwan [11] to validate their simulation model. Similarly, the same theory was used to validate the simulation model for the present work. The equation for the water jet velocity at the orifice can be obtained using the following theoretical formulation.

Theoretical waterjet velocity, V_{th}:

$$V_{th} = \sqrt{\frac{2p}{\rho}} \quad (1)$$

Compressibility of water:

$$\frac{\rho}{\rho_\circ} = \left(1 + \frac{P}{L}\right)^n \quad (2)$$

Where p is the operating pressure, ρ is water density (kg/m3), L = 345 Mpa and n = 0.162 at 25^0 C. Note that value of L depends on the pumping pressure of the AWJ machine for the pump plunger to pumped before any water begins to exit the check valve.
The resulting equation for the waterjet velocity:

$$V_j = \sqrt{\sqrt{\frac{2L}{(1-n)\rho_0}\left[\left(1 + \frac{P}{L}\right)^{1-n} - 1\right]}} \quad (3)$$

Compressibility factor:

$$\varphi = \sqrt{\frac{V_j}{V_{th}} = \sqrt{\frac{L}{P\ (1-n)}\left[\left(1 + \frac{P}{L}\right)^{1-n} - 1\right]}} \quad (4)$$

The waterjet velocity can then be expressed in the following equation:

$$V_J = C_d \varphi V_{th} \quad (5)$$

Where discharge coefficients, $C_d = 0.85$. The value is based on the function of the jet size from past research [11].
Using the particle erosion and accretion method to enables erosion rates to be monitored at wall boundaries. The erosion rate equation is defined as below:

$$R_{erosion} = \sum_{p=1}^{n} \frac{\dot{m}_p C(d_p) f(a) v^{b(v)}}{A_{face}} \quad (6)$$

Where $C(d_p)$ is a function of particle diameter,a is the impact angle of the particle path with the wall face, $f(a)$is a function of impact angle, v is the relative particle velocity, $b(v)$ is a function of relative particle velocity, and A_{face} is the area of the cell face at the wall. Default values are $C = 1.8 \times 10^9$, $f = 1$, and $b = 0$. The erosion rate density is presented in the unit of kg/s/m^2, noted that this value just represent the qualitative value and not the physical value which reflect the actual materials being used.
K-ε turbulence model is used to simulate turbulence for mixed flow of water, air and abrasive of an AWJ process. The turbulence quantity is specified using the Percentage Intensity, I, which is defined as the root-mean-square of the velocity fluctuations, u', to the mean velocity $u_{average}$. The value of the turbulence intensity specified at water pressure inlet boundary conditions are defined as below:

$$I = \frac{u'}{u_{average}} = 0.16(Re_{Dh})^{-1/8} \quad (7)$$

The Reynold's number, Re, for given size of the hydraulic diameter, D_h, of the AWJ waterjet circular tube were obtained using the following equation:

$$Re_{Dh} = \frac{\rho u D_h}{\mu} \quad (8)$$

Where, Re is Reynolds number (non-dimensional), u is velocity based on the actual cross section area of the duct or pipe (m/s), μ is the dynamic viscosity (Ns/m^2) and L is the characteristic length (m) and ν is the kinematic viscosity (m^2/s).

2. Geometry and Parameters

The numerical model is based on the 3-D model of commercial AWJ cutting head from past research [11], [12]. The geometrical and parameters are defined as shown in table 1. The material properties for the nozzle and the abrasives are shown in table 2 and 3 respectively. High pressured waterjet and abrasive is released from their corresponding inlet and mixed into the mixing chamber where entrainment occurs and focused to the nozzle tube and eventually released. The model was then meshed using the standard meshing in FLUENT 15.0. The wall of the nozzle is meshed using inflation by selecting the surface selection option to simulate wall interaction with the fluid flow.

(a) (b)

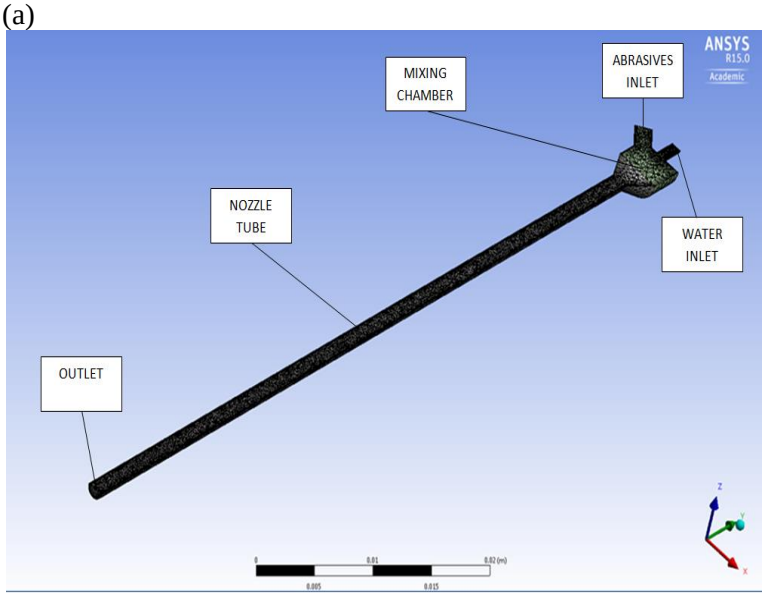

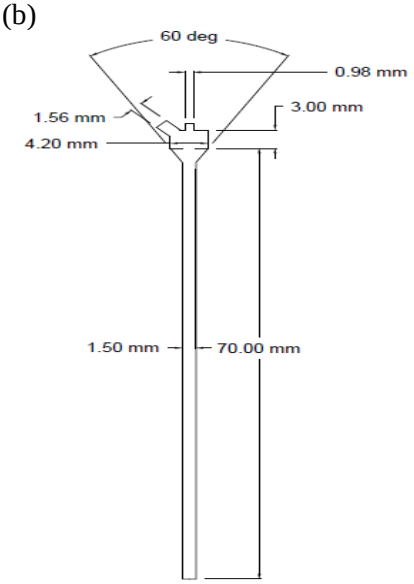

Figure 1. Schematics of the Cutting head (a) Geometry parameters designations (b) Geometry values.

Table 1. Boundary condition and parameter values.

Parameters	Typical Values
Nozzle length (mm)	50.8
Nozzle inlet angle (^{0})	60^0
Nozzle diameter (mm)	1.14
Orifice diameter (mm)	0.38
Water pressure (Mpa)	310
Abrasive flow rate (g/s)	3.8
Mesh size (#)	80# (0.177 mm)

Table 2. Nozzle material properties.

Material	Density (kg/m^3)	Specific Heat, Cp (J/kg-k)	Thermal Conductivity
Tungsten Carbide	15680	39.8	110

Table 3. Abrasives material properties.

Material	Density (kg/m^3)	Specific Heat, Cp (J/kg-k)	Thermal Conductivity
Aluminium Oxide (al2o3)	3950	880	-

Table 2 shows the parameters for boundary conditions. The shape factor is a parameter for the abrasive particles irregularity. A shape factor of 1.0 signifies a particle with a circular shape and decrease of value signifies increase of irregularity. The typical value for particle mesh size chosen was 80 or approximately 0.1 mm in diameter and is assumed to be uniform for simplification of the solution.

3. Results and Discussion

The geometry of the nozzle were set and mesh methods were generated. In figure 2 (a) shows the assembly methods for Quadrilateral mesh which mainly partition the parts to four sides cell shape. Figure 2 (b) shows the mesh generated by the Cutcell assembly methods which the areas zone were partitioned to almost exact cubic shaped. It simplified when dealing with tubular zone. Figure 2 (c) shows the mesh generated by tetrahedrons methods which are observed to be very fine in details. Tetrahedrons partitioned the zones to four vertices, six edges and bound to four triangular faces.

(a)

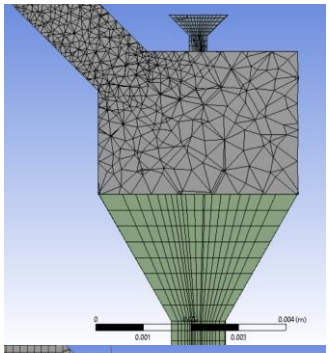

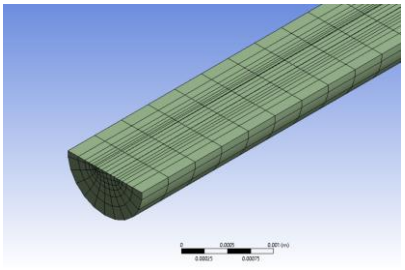

(b)

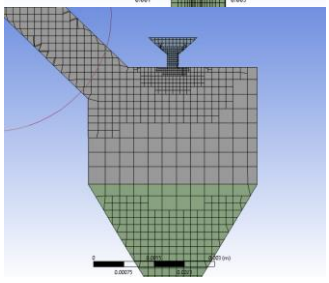

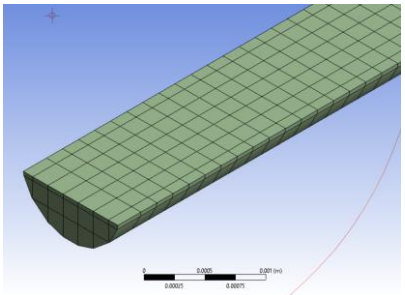

(c)

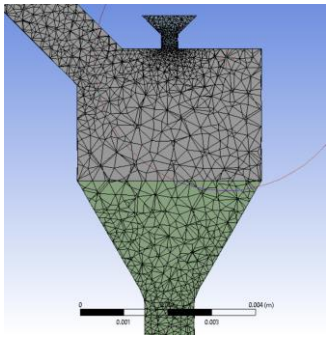

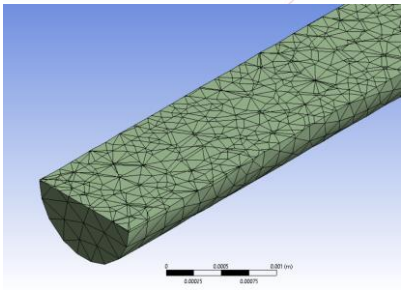

Figure 2. Meshing structure of Quadrilateral mesh (a), Cutcell mesh (b) and Tetrahedrons mesh (c).

Table 4 shows the comparison of the assembly methods in term of the cell size, nodes, number of elements, processing time, convergence quality and the adjusted under relaxation factor (URF). The cell size was adjusted to be equal so that the comparison will be relevant. However, there were some limitations to ensure the same cell size as the software automatically adjusted the value to prevent ratio error. Therefore, the cell size has been to be as close as possible which also includes the number of nodes and elements. The simulation were done by comparing different nozzle size and compared with results of past studies [12]. In term of processing time, the Quadrilateral mesh methods is the fastest followed by Cutcell and Tetrahedrons methods, respectively. This is mainly due to cell size which is less fine compared to tetrahedrons which took around seven days for a simulation to complete [18]. The simulations tend to diverged more for both Cutcell and Tetrahedrons which shows that the meshing methods proved to be difficult for complex structure and multiphase flow. The URF were also adjusted to negate the divergence problem.

Table 4. Comparison of different Assembly Methods in term of Processing time, Convergence Quality and Under Relaxation Factor (URF).

Assembly Methods	**Quadrilateral**	**Cut cell**	**Tetrahedrons**
Min Size	3.03E-05	4.69E-05	4.69E-05
Max Face Size	3.03E-03	6.07E-03	6.07E-03
Nodes	22205	26037	20416
Elements	30482	23682	95680
Processing time	3 Days	3 – 4 Days	7 Days
Convergence Divergence	Converged Well and rarely diverged	Divergence is Prevalent	Divergence is Prevalent
Under Relaxation Factor	None	Minimal	High

Figure 3 shows the effect of nozzle length with the erosion wear rate. It is revealed that the length of the nozzle has a direct influence on the nozzle wear rate. However, the simulated nozzle wear shows varied results as the length of the nozzle increases. In table 5, the information of the nozzle rate presented in (kg/m^2-s) and the accuracy between the simulated and the experimental erosion rate in percentage were revealed. The Quadrilateral meshing shows the closest accuracy out of the other assembly methods. This is followed by Tetrahedral with a minor accuracy difference between Quadrilateral mesh and Cut Cell assembly which have major differences in accuracy. It also presented that Quadrilateral meshing have a consistent trend with the actual erosion rate in which the erosion rate declines as the length of the nozzle increases. The Tetrahedral assembly have a considerable accuracy at the beginning nozzle value of 32.5 mm. The erosion wear however had increased it erosion rate value when nozzle was increased to 50.8 mm. The erosion rate value reduced again as the length increases. Whereas for Cut Cell mesh assembly, a contrasting value were shown when the nozzle length is at value of 32.5 mm. The erosion rate begins to be decrease in trend but were slightly inconsistent as the length increases. Given the parameters of length is concerned, the Quadrilateral assembly shows considerable accuracy and consistent trend of erosion rate value and trend. General pattern indicates that the erosion of nozzle decreases as the nozzle length increases which is similar to results acquired in past experimental results [12],[19],[20].

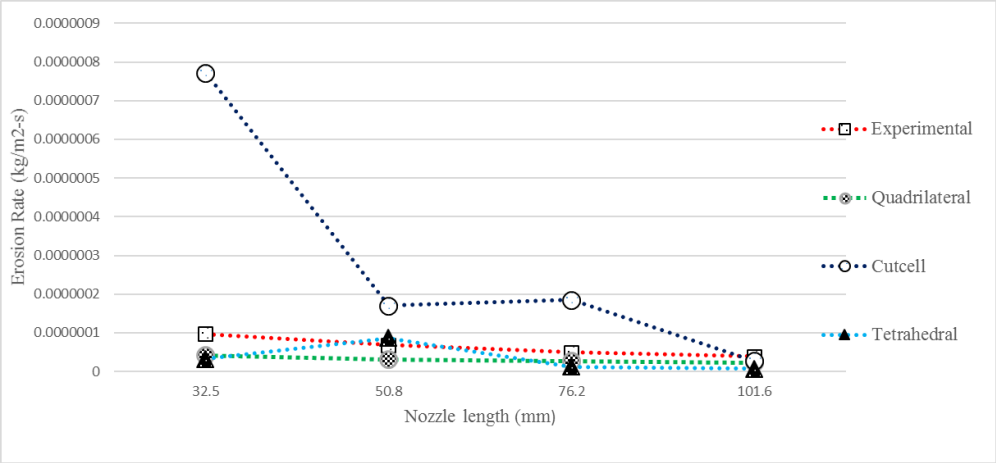

Figure 3. Effect of Nozzle length on erosion wear.

Table 5. Comparison of Assembly methods in term of nozzle length.

Experimental model		**Quahedral**		**Cut cell**		**Tetrahedral**	
Nozzle length (mm)	**Erosion Rate (kg/m2-s)**	**Erosion rate (kg/m2-s)**	**Accuracy (%)**	**Erosion rate (kg/m2-s)**	**Accuracy (%)**	**Erosion rate (kg/m2-s)**	**Accuracy (%)**
32.5	9.723E-08	4.078E-08	-58%	7.722E-07	694%	3.261E-08	-66%
50.8	6.802E-08	3.180E-08	-53%	1.701E-07	150%	8.670E-08	27%
76.2	4.918E-08	2.621E-08	-47%	1.854E-07	277%	1.290E-08	-74%
101.6	3.907E-08	2.315E-08	-41%	2.676E-08	-31%	6.588E-09	-83%

4. Conclusion

In summary, different assembly method of meshing was generated and simulated to solve the AWJ nozzle erosion. Out of the three methods, the Quadrilateral mesh showed promising results in term of processing time, convergence quality and erosion rate accuracy followed by Cutcell and Tetrahedrons mesh, respectively. The Cutcell and Tetrahedrons methods requires significant processing time and are prevalent in encountering divergence which eventually leads to repetitions of simulation. It also required to adjust the URF which will affect the accuracy of the calculation. Therefore, it is suggested that the simulation to be proceed using the Quadrilateral mesh method.

Acknowledgement

The authors would like to gratefully acknowledge the financial support from the Universiti Malaysia Pahang (UMP) Research Grant (RDU150347).

References

[1] Blazek J 2005 *Computational Fluid Dynamics: Principles and Applications:(Book with accompanying CD)*: Elsevier
[2] Versteeg H K and Malalasekera W 2007 *An introduction to computational fluid dynamics: the finite volume method*: Pearson Education

[3] Anderson J D and Wendt J 1995 *Computational fluid dynamics* vol 206: Springer
[4] Azhari A, Schindler C, Kerscher E and Grad P 2012 *The International Journal of Advanced Manufacturing Technology* **63** 1035-46
[5] Folkes J 2009 *Journal of Materials Processing Technology* **209** 6181-9
[6] Momber A W and Kovacevic R 2012 Springer Science & Business Media)
[7] Junkar M, Jurisevic B, Fajdiga M and Grah M 2006 *International Journal of Impact Engineering* **32** 1095-112
[8] Maniadaki K, Kestis T, Bilalis N and Antoniadis A 2007 *The International Journal of Advanced Manufacturing Technology* **31** 933-40
[9] Deepak D, Anjaiah D, Karanth K V and Sharma N Y 2012 *Advances in Mechanical Engineering* **4** 186430
[10] Baisheng N I E, Hui W, Lei L I, Jufeng Z, Hua Y, Zhen L I U, Longkang W and Hailong L 2011 *Procedia Engineering* **26** 48-55
[11] Mostofa M G, Kil K Y and Hwan A J 2010 *Journal of mechanical science and technology* **24** 249-52
[12] Nanduri M, Taggart D G and Kim T J 2002 *International Journal of Machine Tools and Manufacture* **42** 615-23
[13] Kamarudin N H, Rao A P and Azhari A 2016 In: *IOP Conference Series: Materials Science and Engineering*: IOP Publishing) p 012016
[14] Hu G, Zhu W, Yu T and Yuan J 2008 In: *Industrial Informatics, 2008. INDIN 2008. 6th IEEE International Conference on*: IEEE) pp 1700-5
[15] Meakhail T A and Teaima I R 2013 *ratio* **2**
[16] Ng E Y-K and Guannan D 2014 *The International Journal of Advanced Manufacturing Technology* **78** 939-46
[17] Zhang H, Han B, Yu X and Ju D 2013 *Shock and Vibration* **20** 895-905
[18] Hosain M L and Fdhila R B 2015 *Energy Procedia* **75** 3307-14
[19] Pi V N and Tuan N Q 2009 In: *Advanced Materials Research*: Trans Tech Publ) pp 345-50
[20] Hashish M 1994 *Journal of tribology* **116** 439-44